Accurate Position Control of a Pneumatic Actuator

Jiing-Yih Lai
Graduate Associate.

Chia-Hsiang Menq
Assistant Professor.
Mem. ASME

Rajendra Singh
Professor.
Mem. ASME

Fluid Power Laboratory,
Department of Mechanical Engineering,
The Ohio State University,
Columbus, Ohio 43210-1107

We propose a new control strategy for on-off valve controlled pneumatic actuators and robots with focus on the position accuracy. A mathematical model incorporating pneumatic process nonlinearities and nonlinear mechanical friction has been developed to characterize the actuator dynamics; this model with a few simplifications is then used to design the controller. In our control scheme, one valve is held open and the other is operated under the pulse width modulation mode to simulate the proportional control. An inner loop utilizing proportional-plus-integral control is formed to control the actuator pressure, and an outer loop with displacement and velocity feedbacks is used to control the load displacement. Also, a two staged feedforward force is implemented to reduce the steady state error due to the nonlinear mechanical friction. Experimental results on a single-degree-of-freedom pneumatic robot indicate that the proposed control system is better than the conventional on-off control strategy as it is effective in achieving the desired position accuracy without using any mechanical stops in the actuator.

1 Introduction

Pneumatic actuation is used extensively for numerous position control applications, but only in the open-loop control mode where the strokes of the moving parts are usually fixed by the mechanical stops. A closed-loop control system is generally not available because of the fundamental problems associated with the air compressibility, poor damping ability, significant mechanical friction, and strong nonlinearities. Nevertheless, it is expected that pneumatic systems under computer control will become more popular to meet the demand of simple and low cost automation. Accordingly, the focus of this paper is on the development of a new control strategy which will overcome some of the difficulties mentioned above.

The transfer function approach has been used historically to model the dynamics of pneumatically actuated systems (Shearer, 1956, 1957; Burrows, 1969; and Botting, 1970). However, such a linearized model is suitable only for the mid-stroke position. Recently, the state space approach has been utilized to extend the linearized model over several operating positions (Scavarda et al., 1987 and Liu et al., 1987). But the effect of mechanical friction has been neglected. Since the servovalves are very expensive and not commonly available, on-off valve controlled pneumatic systems are typically used in the industry. Using these, full power can be utilized to drive the load, but the precise position accuracy can not be obtained. Such systems have been studied both analytically (Burrows, 1967 and Bowns et al., 1972) and experimentally (Eun et al., 1982, 1984).

Pulse width modulation offers considerable advantages in the control of dc motors and hydraulic servos as it can reduce the effects of nonlinearities such as hysteresis, threshold, stiction, dead-zone and null shift, and improve the system reliability and performance. Such a technique has also been applied to on-off controlled pneumatic systems by Noritsugu (1985, 1987) and Morita (1985). Noritsugu (1987) employed three on-off valves for a particular motion control problem where the two valves were under on-off control, and the third valve (automotive injection valve) was under the PWM control when operating in the vicinity of the desired position. Linearized analysis was used to study the effect of various parameters including friction on the system response. But this scheme is too complex and expensive. Also, no efficient method can be used to determine some of the parameters in the controller such as the selection of switch points to change the valve motion and the position feedback gain. Accordingly, this strategy can not be applied in practice. Morita (1985) and Noritsugu (1985) have also implemented the PWM mode in pneumatic manipulators to control pressure and contact force, respectively; both have demonstrated that a continuous feedback control of pressure and grasping force can be obtained with this technique without using any servovalve.

2 Objectives and System Description

Based on the literature review, it is evident that most of the control strategies available for position control are still not satisfactory. Some of the designs are suitable only for low position accuracy; others are so complex that it is difficult to determine the control gains or system parameters when applied to a multidegree of freedom system. To overcome such deficiencies typically evident in the literature and to develop accurate pneumatic manipulators, we establish two major objectives. First, a comprehensive nonlinear model is developed to characterize the actuator dynamics. It is supported by a computer simulation study. Second, we intend to develop a

Contributed by the Dynamic Systems and Control Division for publication in the JOURNAL OF DYNAMIC SYSTEMS, MEASUREMENT AND CONTROL. Manuscript received by the Dynamic Systems and Control Division August 18, 1988; revised manuscript received April 1989. Associate Editor: D. Hullender.

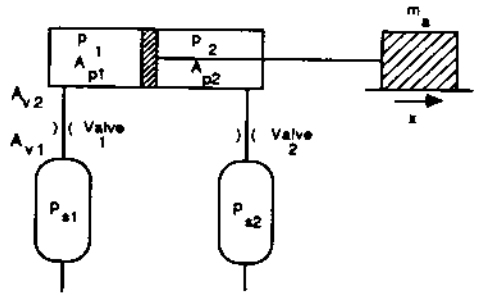

Fig. 1 Schematic of the pneumatic system. Here, p_1 and p_2 are chamber pressures, A_{p1} and A_{p2} are cross-sectional areas, A_{v1} and A_{v2} are orifice areas associated with the input and output ports of valve 1, p_{s1} and p_{s2} are supply pressures, m_a is the load and x is the actuator-load displacement.

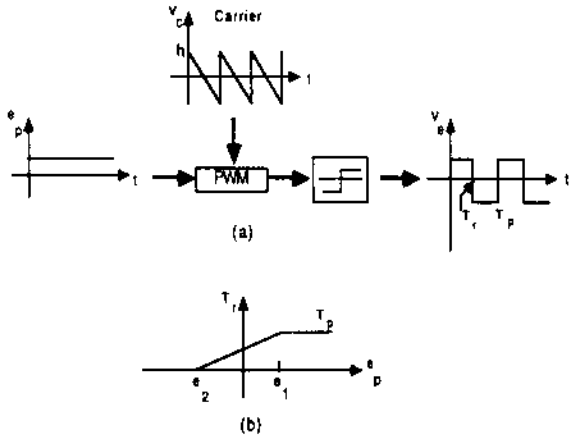

Fig. 2 Pulse width modulator (PWM) applied to valve 1. (*a*) Formulation of the PWM signal. (*b*) Duty pulse width T_r versus pressure error e_p. Here v_s is the voltage input to valve 1, v_c is carrier signal, h is the pulse magnitude of the carrier, T_p is the pulse period, T_r is the pulse width when valve 1 is open, t is time and e_1 and e_2 are pressure errors.

novel control strategy using the on-off valves to achieve high position accuracy. A simplified analytical model is formulated to design the control system. Successful experimental implementation on a single degree of freedom pneumatic robot is demonstrated. This paper essentially presents the first progress report on a comprehensive research project at the Ohio State University on the dynamics and control of multidegree of freedom pneumatic manipulators.

The system, as schematically shown in Fig. 1, is composed of two on-off valves in conjunction with a linear actuator carrying an external load m_a. For control purposes, it is assumed that the displacement x, velocity $\dot{x}$, and the chamber pressures $p_1(t)$ and $p_2(t)$ can be measured. To reduce the nonlinearity associated with large pressure variation, we propose to hold the valve 2 open such that $p_2(t)$ remains nearly equal to supply pressure p_{s2}. This can be achieved physically by connecting a large accumulator tank to the air supply port of valve 2. Valve 1 is under the PWM mode control, where a periodic pulse signal $v_c(t)$ with duty pulse width T_r being proportional to the pressure error e_p (pressure difference between actual and command pressure in chamber 1) is input to the solenoid of valve 1. Figure 2(*a*) illustrates the formulation of the PWM signal, and Fig. 2(*b*) shows the design of duty pulse width T_r versus e_p. Note that when $e_p > e_1$, valve 1 is open for the whole period, and it is closed when $e_p < e_2$.

3 Analytical Models

3.1 Nonlinear Model. The following assumptions are made: (i) the ideal equation of state is valid, (ii) the thermofluid processes are isentropic, and (iii) the bandwidth of the valves is larger than that of the actuator-chamber dynamics. The last assumption should allow us to determine the dynamics of the whole system as the combination of chamber dynamics and load dynamics. Note that the pressure dynamics of chamber 2 is ignored as $p_2(t) \approx p_{s2}$. The governing equations for chamber 1 are developed as follows.

$$p_1(t)V_1(t) = m_1(t)RT_1(t) \tag{1}$$

$$p_1(t)T_1(t)^{n/(1-n)} = p_{10}T_{10}^{n/(1-n)},\ p_{10} = p_1(0),\ T_{10} = T_1(0) \tag{2}$$

where V_1 is the volume 1, m_1 is the mass 1, R is gas constant, T_1 is temperature, and n is the isentropic constant ($n = 1.4$ for air). Using equations (1) and (2), we get

$$\dot{p}_1(t)V_{10} + \dot{p}_1(t)A_{p1}x(t) + np_1(t)A_{p1}\dot{x}(t) - n\dot{m}_1(t)RT_{10}\left(\frac{p_1(t)}{p_{10}}\right)^{(n-1)/n} = 0$$

$$V_1(t) = V_1(0) + A_{p1}x(t),\ V_1(0) = V_{10} \tag{3}$$

The mass flow rate $\dot{m}_1$ in equations (3) can be expressed as follows (Andersen, 1967):

$$\dot{m}_1 = \begin{cases} C_{d1}A_{v1}p_{s1}N_{12}K\sqrt{T_{10}} & ,\ v_e(t) > 0 \\ -C_{d2}A_{v2}p_4C_{24}K\left(\dfrac{p_1(t)}{p_{10}}\right)\sqrt{\dfrac{n-1}{n}} & ,\ v_e(t) < 0 \end{cases} \tag{4}$$

$$N_{12} = \begin{cases} k_n\left[\left(\dfrac{p_1(t)}{p_{s1}}\right)^{2/n} - \left(\dfrac{p_1(t)}{p_{s1}}\right)^{(n+1)/n}\right]^{1/2} & ,\ \dfrac{p_1}{p_{s1}} > r_c, r_c = 0.528 \text{ for air} \\ 1 & ,\ \dfrac{p_1}{p_{s1}} < r_c \end{cases}$$

$$C_{24} = k_n\left(\frac{p_4}{p_1(t)}\right)\left[\left(\frac{p_4}{p_1(t)}\right)^{2/n} - \left(\frac{p_4}{p_1(t)}\right)^{(n+1)/n}\right]^{1/2}$$

$$K = \left[\frac{ng}{R}\left(\frac{2}{n+1}\right)^{\frac{n+1}{n-1}}\right]^{1/2}$$

$$C_{d1} = C_{a1} - C_{b1}\left(\frac{p_1(t)}{p_{s1}}\right),\ C_{d2} = C_{a2} - C_{b2}\left(\frac{p_1(t)}{p_4}\right)$$

where p_4 is the atmospheric pressure, k_n is a constant, 0.2588 for air and g is the gravitational constant. The discharge coefficients C_{d1} and C_{d2} are defined with respect to the input and output ports of valve 1, respectively, and are modeled as a function of pressure ratio (p_1/p_{s1}) with coefficients C_{a1}, C_{b1}, and C_{a2}, C_{b2}, respectively. Here $C_{a1} = 0.503$, $C_{b1} = 0.001$, $C_{a2} = 0.231$ and $C_{b2} = 0.121$. It is noted that when $v_e(t) > 0$, air flows from the supply pressure p_{s1} port through one orifice of the valve to the actuator; conversely when $v_e(t)$ is negative, air flows out from the actuator through another orifice of the valve to the atmosphere. The sign of mass flow rate $\dot{m}_1$ changes as the valve spool moves from one orifice to another. The actuator-load dynamics is given as follows:

$$m_a\ddot{x} = F_p(t) - F_d(t),$$

$$F_p(t) = A_{p1}(p_1(t) - p_4) - A_{p2}(p_2(t) - p_4)$$

$$F_d(t) = \begin{cases} F_c\,\mathrm{sgn}(\dot{x}) & ,\ \dot{x} \neq 0 \\ F_p(t) & ,\ \dot{x} = 0,\ F_p(t) < F_s \\ F_s\,\mathrm{sgn}(F_p(t)) & ,\ \dot{x} = 0,\ F_p(t) > F_s \end{cases} \tag{5}$$

where $F_p(t)$ is the external force acting on the piston, $F_d(t)$ represents the mechanical friction, F_c is the Coulomb friction

coefficient, and F_s is the stiction coefficient. This equation shows that the acceleration $\ddot{x}$ is mainly affected by pressures p_1 and p_2. However, due to the system nonlinearity, it is difficult to control p_1 and p_2 at the same time. Our approach in keeping p_2 nearly constant should reduce the system nonlinearity significantly.

3.2 Simplified Analytical Model. As we can see from equations (3) to (5), the nonlinear characteristics of this system are primarily due to the air compressibility, valve flow rate, and the mechanical friction. Here we develop a simplified analytical model to understand the dynamics better and to design the controller. The conventional approach linearizes the system around the equilibrium position assuming that the load displacement $x(t)$ is small (Shearer, 1956; Andersen, 1967; and Burrows 1969). We deviate from this by linearizing the nonlinear equations (3) to (5) around the command displacement x_d. This should enable us to design the controller such that when the actuator-load is in the vicinity of x_d, the load displacement x should converge to x_d quickly. First we examine the characteristics of PWM mode.

3.2.1 Transfer Characteristics of PWM. Our method employs a double Fourier series expansion in two variables (Black, 1953). Consider that the signal input $v_e(t)$ to the pulse-width modulator is given by $V_0 \sin \omega t$ where V_0 is the amplitude and ω is the modulating frequency. The modulated signal $u(\omega t, \omega_c t)$ of carrier frequency ω_c can be expressed as follows:

$$u(\omega t,\omega_c t) = \frac{1}{2} A_{00} + \sum_{n=1}^{\infty} [A_{0n}\cos n\omega t + B_{0n}\sin n\omega t] + \sum_{m=1}^{\infty} [A_{m0}\cos m\omega_c t + B_{m0}\sin m\omega_c t] + \sum_{m=1}^{\infty} \sum_{n=\pm 1}^{\pm\infty} [A_{mn}\cos(m\omega_c t + n\omega t) + B_{mn}\sin(m\omega_c t + n\omega t)] \quad (6)$$

Also, since $u(\omega t,\omega_c t)$ is a square wave, it can be given by

$$u(\omega t, w_c t) = \begin{cases} A_{v1} & , 0 \le \omega_c t \le \left(\pi + \frac{\pi}{h} V_0 \sin\omega t\right) \\ -A_{v2} & , \left(\pi + \frac{\pi}{h} V_0 \sin\omega t\right) \le \omega_c t \le 2\pi \end{cases} \quad (7)$$

where h is the amplitude of the carrier, as shown in Fig. 2(*b*). By substituting equation (6) into equation (7), all of the coefficients A_{mn} and B_{mn} can be evaluated. All cosine coefficients A_{mn} vanish because the input is a sine function. The *dc* gain A_{00} and the first few terms of B_{mn} are given below.

$$A_{00} = A_{v1} - A_{v2},$$

$$B_{01} = \frac{\beta V_0}{2\pi}(A_{V1} + A_{V2}),\ B_{0n} = 0,\ n = 2,3,\ldots,$$

$$B_{10} \doteq \frac{A_{V1} + A_{V2}}{2\pi^2}\left(\int_0^{2\pi} 1 + \cos\left(\frac{\pi}{h} V_0 \sin\omega t\right) d(\omega t)\right),$$

$$B_{20} = \frac{A_{V1} + A_{V2}}{4\pi^2}\left(\int_0^{2\pi} 1 - \cos\left(2\frac{\pi}{h} V_0 \sin\omega t\right) d(\omega t)\right), \quad (8)$$

Thus, the modulated signal $u(\omega t, \omega_c t)$ in equation (6) is reduced to

$$u(\omega t,\omega_c t) = \frac{1}{2} A_{00} + B_{01}\sin\omega t + \sum_{m=1}^{\infty} B_{m0}\sin m\omega_c t + \sum_{m=1}^{\infty} B_{m1}\sin(m\omega_c t \pm \omega t) \quad (9)$$

The frequency component of the second term corresponds to the frequency component of the input signal. The third term separates into frequencies corresponding to the carrier frequency ω_c and to the harmonics of this frequency. The frequency components of the last term correspond to the sum and difference of the modulating frequency ω and integral multiples of the carrier frequency ω_c. Equations (8) and (9) show that as ω_c or V_0 is increased, the effect of the modulation is decreased.

3.2.2 Chamber and Load Dynamics. To simplify the mathematical model, the motion terms x, $\dot{x}$, and $\ddot{x}$ are linearized around the command position x_d, but the pressure p_1 is not linearized which should enable us to include the nonlinear mechanical friction. Further we assume that the variation of temperature is small, i.e., $T_1(t) \approx T_{10}$. This assumption has been used by several previous investigators (Shearer, 1957; Burrows et al., 1967; and Noritsugu, 1987). Also, it seems to be valid in our laboratory experiment. Accordingly equation (3) is simplified to yield

$$\dot{m}_1 = k_3\dot{p}_1 + k_4\dot{x}_p,\ k_3 = \frac{\bar{V}_1}{nRT_{10}},\ k_4 = \frac{\bar{p}_1 A_{p1}}{RT_{10}} \quad (10)$$

where x_p represents the perturbation of x around the command position, $\bar{V}_1$ represents the equilibrium volume, and the operating pressure $\bar{p}_1$ is defined as the average pressure for each cycle of valve motion in the command position. Linearizing equation (4) for $\dot{m}_1$, we get

$$\dot{m}_1 = -k_1 p_1 + k_2 A_v \quad (11)$$

$$A_v = A_{v1},\ v_e(t) > 0;\ A_v = -A_{v2},\ v_e(t) < 0$$

$$k_1 = \begin{cases} A_{v1}\left[\frac{C_{b1}}{p_{s1}}(\bar{N}_{12} + n_{12p}\bar{p}_1) - C_{a1}n_{12p}\right] & , v_e(t) > 0 \\ A_{v2}\left[\frac{C_{b2}}{p_{s1}}(\bar{C}_{24} + c_{24p}\bar{p}_1) - C_{a2}c_{24p}\right] & , v_e(t) < 0 \end{cases}$$

$$k_2 = \begin{cases} C_{b1}n_{12p}\bar{p}_1^{\,2}/p_{s1} + C_{a1}(\bar{N}_{12} - n_{12p}\bar{p}_1) & , v_e(t) > 0 \\ C_{b2}c_{24p}\bar{p}_1^{\,2}/p_{s1} + C_{a2}(c_{24p}\bar{p}_1 - \bar{C}_{24}) & , v_e(t) < 0 \end{cases}$$

where $\bar{N}_{12}$ and $\bar{C}_{24}$ represent the operating values and n_{12p} and c_{24p} are the perturbation of N_{12} and C_{24} around the operating pressure, respectively. Combining equations (10) and (11), one has

$$\tau\dot{p}_1 + p_1 = k_a A_v - k_b\dot{x}_p,\ \tau = k_3/k_1,\ k_a = k_2/k_1,\ k_b = k_4/k_1 \quad (12)$$

Equation (12) represents the pressure dynamics of chamber 1 around the equilibrium position, which is similar to a first order system, but with distinct gains depending on the direction of fluid flow. The equation for load dynamics is given by modifying equation (5) around the command position x_d as

$$m_a\ddot{x}_p = A_{p1}p_1 - F_t - F_d(t),\ F_t = A_{p1}p_4 + A_{p2}(p_2 - p_4) \quad (13)$$

Equations (12) and (13) represent the simplified model for the system. Note that this model is similar to a linear model except for the friction term $F_d(t)$ and the time-varying gains $k_a(t)$, $k_b(t)$, and $\tau(t)$ which vary according to $v_e(t)$. However, since the value is operated in the PWM mode, the high-frequency switching of the pulse-width-modulated wave and the resulting dither effect can reduce the effect of nonlinear friction and gain variations. To analyze the effect of $k_a(t)$, $k_b(t)$, and $\tau(t)$, first it is necessary to determine $\bar{p}_1$ from the steady state considerations.

$$\bar{p}_1 = [A_{p2}p_2 + (A_{p1} - A_{p2})p_4 + \bar{F}_d]/A_{p1} \quad (14)$$

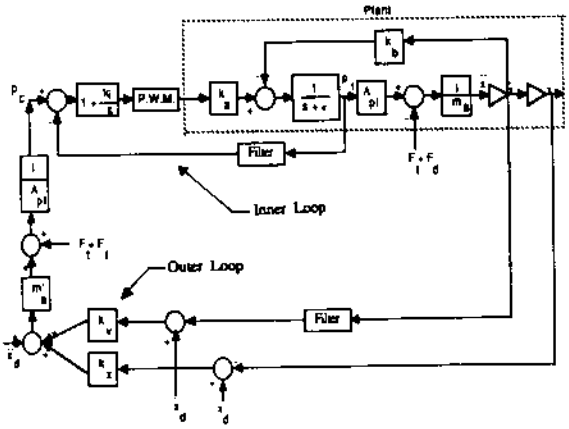

Fig. 3 Proposed control strategy

$$\bar{F}_d = \int_t^{t+T_p} F_d(t)dt = \int_t^{t+T_p} A_{p1}(p_1(t) - p_4)dt - \int_t^{t+T_p} A_{p2}(p_2 - p_4)dt \quad (15)$$

where $\bar{F}_d$ represents the average friction acting on the load associated with each cycle of valve motion in the steady state. This equation shows that if $\bar{F}_d$ is a constant, $\bar{p}_1$ is a constant too and does not depend on the command position x_d. Also, the effect of average friction is reduced. Since $k_a(t)$, $k_b(t)$, and $\tau(t)$ are very sensitive to the operating pressure $\bar{p}_1$ as evident by equations (10)–(12), a uniform operating pressure over all equilibrium positions ensures that these parameters do not vary much for different piston positions. But if $\bar{p}_1$ changes with the piston position, then the system parameters and feedback gains would have to be position dependent. For instance consider the case when only one valve is used to control the pressure difference across the chamber. Now p_2 would be unsteady and position dependent, and hence $\bar{p}_1 = \bar{p}_1(x)$; also it would be very difficult in this case to determine the operating pressure. Further, note that among the parameters k_1, k_2, k_3, and k_4 in equations (10) and (11), only k_3 is affected by the piston location. Accordingly, the major control issue here is how to reduce the effect of k_3 and hence of τ on the pressure dynamics.

4 Proposed Control Strategy

Figure 3 illustrates the proposed control block diagram for the system. The closed-loop system is composed of two loops: (i) an inner loop involving pressure feedback to control the pressure p_1, (ii) an outer loop involving both displacement x and velocity $\dot{x}$ feedbacks to control x. Given the desired displacement x_d, velocity $\dot{x}_d$ and acceleration $\ddot{x}_d$, the outer loop computes the desired pressure needed to move the load m_a and the inner loop controls the actual pressure response to match the desired one. The inner and outer loops are almost independent of each other except for the k_b term which couples the chamber dynamics and load dynamics. To analyze the closed-loop system behavior, we neglect the effect of filter dynamics and assume that the carrier frequency ω_c is sufficiently large such that the effect of the carrier signal is small. Hence the transfer characteristic of the pulse-width modulator can be expressed as a pure gain.

(*a*) *Inner Loop Control:* The open-loop dynamics of the inner loop as shown in Fig. 3 is described as:

$$p_1 = \frac{k_a k_w (s + k_i)}{s(s+\tau)} p_c + k_b \dot{x}_p, \quad k_w = \frac{1}{2h}(A_{v1} + A_{v2}) \quad (16)$$

where s is the Laplace variable and k_i is the integral gain. The first term in equation (16) shows that the system is a Type 1 system, and hence the steady-state error is zero for a step input. The second term acts as a disturbance, but it does not affect the steady-state error if x_d is a step input. However, if x_d is a ramp input, a feedforward term proportional to $\dot{x}_d$ has to be added to the controller to compensate the disturbance. We note that as h is decreased, the closed loop time constant can be improved by designing the system such that the response of the inner loop is faster than that of the outer loop; this should ensure that the chamber dynamics does not affect the load dynamics.

(*b*) *Outer Loop Control:* Assume that the inner-loop time constant is much faster than the outer-loop bandwidth, and accordingly the inner-loop dynamics can be neglected. Further, if we let the estimated inertia m_a' as shown in Fig. 3 to be equal to m_a, then the dynamic equation for the error $e(t) = x_d - x(t)$ is

$$\ddot{e} + 2\zeta\omega_n \dot{e} + \omega_n^2 e = 0, \; k_x = \omega_n^{1/2}, \; \zeta = k_v/2\omega_n \quad (17)$$

Equation (17) represents the error dynamics for the closed-loop system with desired natural frequency ω_n and damping ratio ζ for the closed-loop system. The poor damping ability in the original open loop system is improved in the closed loop by using the velocity feedback k_v.

(*c*) *Friction Compensation:* Since it is usually difficult to predict the nonlinear friction accurately, a two staged feedforward force F_f is defined to compensate the friction force as

$$F_f = \begin{cases} \alpha F_c \operatorname{sgn}(\Delta x) & , \; |\Delta x| > \delta \; ; \; \Delta x = x_d - x \\ 0 & , \; |\Delta x| < \delta \end{cases} \quad (18)$$

where α is a scale factor and δ is a threshold value. The damping ratio ζ is set to 1 (critical value) so that when the actual response $x \to x_d$, $\dot{x} \to 0$. Since the feedforward force F_f is switched to zero at this point, the moving part should stick.

(*d*) *Filter Design:* The velocity $\dot{x}$ and pressure p_1 feedback signals should oscillate under the PWM mode whenever a periodic voltage is input to the solenoid of valve 1. Since only the average velocity and pressure are to be controlled, digital filters must be used to remove the high frequency components in the data which are primary due to the periodic spool motion in valve 1. Here, each digital filter is modeled as a first order system with cut-off frequency f_s.

Key features of our proposed control strategy are as follows: (i) since the system is divided into two loops, a better understanding of the process dynamics and control is obtained, (ii) velocity and displacement gains (k_v and k_x) can be used to shift the poles of the load dynamic system to the desired locations, (iii) the amplitude h of the carrier signal u can be used to improve the closed loop time constant of the chamber dynamics such that the chamber response $p_1(t)$ is always faster than the load response $x(t)$, and (iv) a two staged feedforward force F_f can be employed to reduce the steady-state error e.

5 Computer Simulation Results

A computer simulation of the control algorithm described in Section 4 is incorporated with the nonlinear model of Section 3.1 to examine the control strategy. Given the command displacement x_d, the controller computes the desired pressure p_c in chamber 1 using the inputs, actual displacement x and velocity $\dot{x}$. The pressure error signal $e_p = p_c - p_1$ is then fed into the PWM mode which drives valve 1. Various parameters and gains used for the computer simulation study are listed below, and the nonlinear mechanical friction $F_d(t)$ is assumed to be given only by the Coulomb friction F_c: m_a = 6.5 Kg, p_4 = 0.1013 MPa, p_{s1} = 0.372 MPa, p_{s2} = 0.209 MPa, A_{p1} = 0.0792 m^2, A_{p2} = 0.0596 m^2, A_{v1} = 2.0E-4 m^2, A_{v2} = 4.452E-

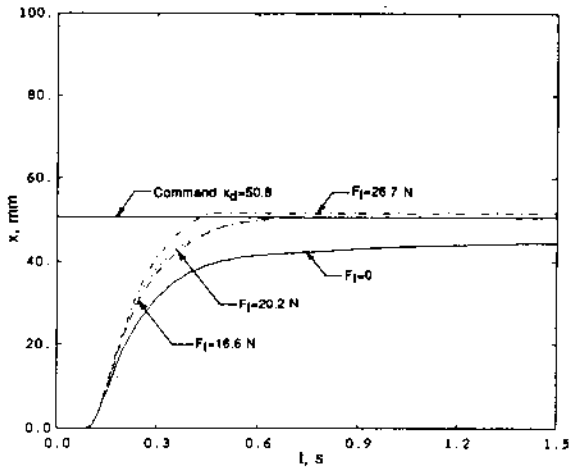

Fig. 4 Effect of feed forward compensation force given Coulomb friction $F_c = 17.78$ N

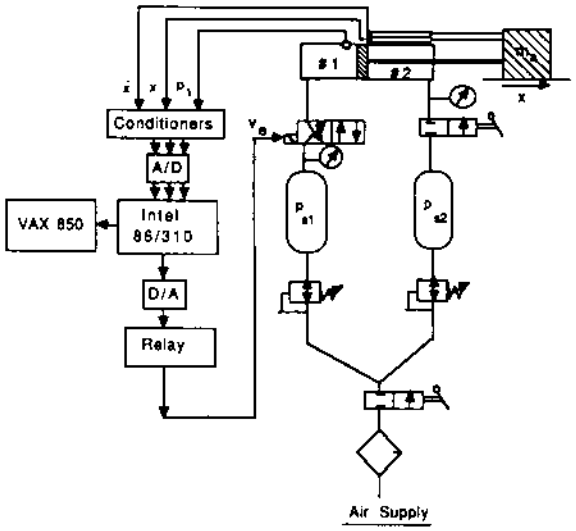

Fig. 5 Experimental schematic. The actuator shown here is the extension/retract arm of the pneumatic robot.

$4\ m^2$, $h = 5.0$, $k_i = 0.1$, $\omega_n = 15.0$ rad/s, $\zeta = 1.0$, $f_s = 40.0$ Hz and $\delta = 2.5E\text{-}4$ m.

Figure 4 illustrates the effect of F_c on the system response which is similar to that of a second order system except for the appearance of time delay initially which is due to that fact that at $t = 0$, $p_2 = p_{s2}$ and $p_{10} = p_4$. Without any compensation force F_f, the steady state error e is large as expected due to the friction. However, as F_f is added to the controller, the steady state error e is reduced substantially. This plot also indicates that the amplitude of F_f is not necessary equal to that of F_c as the moving parts may stick at the same position for many values of F_f.

6 Pneumatic Robot Experiment

A commercial pneumatic robot with five degrees of freedom (Schrader Bellows #MM2) is used for the experimental study. This robot was originally designed only for open-loop control mode. Our experimental set-up is shown in Fig. 5 where only the extension/retract degree of freedom of the robot arm is studied as the example actuator. One port of the arm actuator is connected to a 3-way poppet valve (Parker #T21025) operated by a solenoid which in turn is controlled by an electronic relay. A tank is connected to the other side of the valve to regulate the supply pressures p_{s1}. The other port of the arm actuator is connected to another tank at pressure p_{s2}. The control routines reside on an Intel 86/310 single board microcomputer which is used with a terminal to control the actuator. A 16 channel A/D module (iSBX311) with a resolution of 2.44 mv is used to get the sensor data from a potentiometer to measure x, a velocity pick-up to measure $\dot{x}$ and a strain gage type pressure transducer to measure p_1. An output channel from the D/A(iSBX328) converter is used to send the output signal through a relay circuit to command the valve motion.

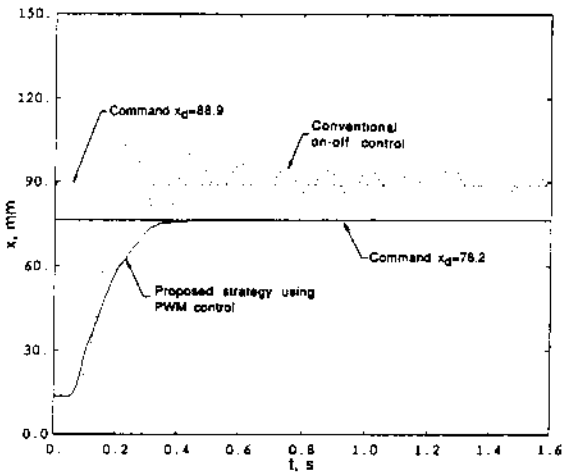

Fig. 6 Comparison of measured step response using two control strategies

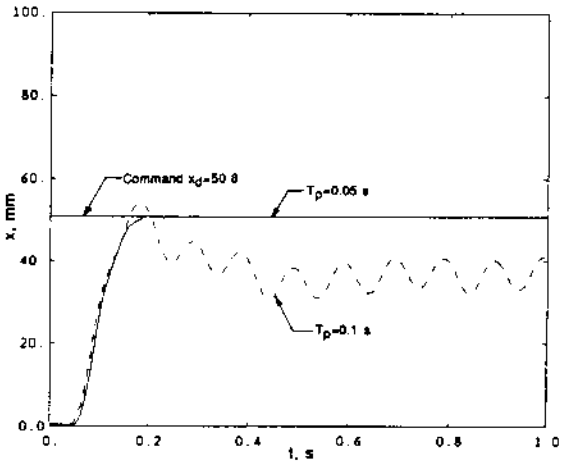

Fig. 7 Effect of the pulse period T_p on the measured step response

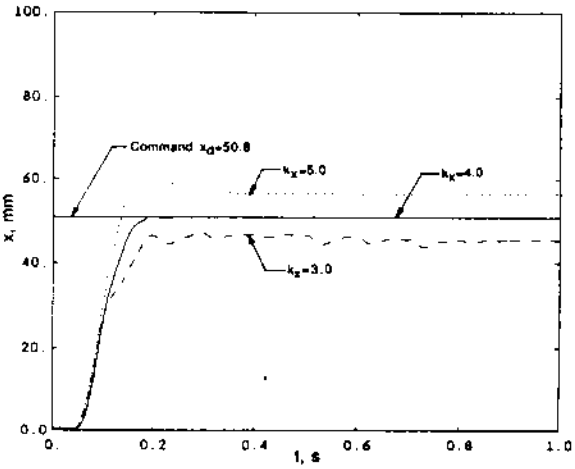

Fig. 8 Effect of position gain k_x on the measured step response

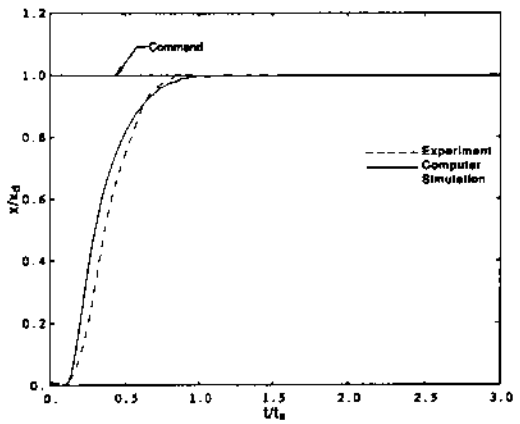

Fig. 9 Comparison between measured and predicted $x(t)$ given step command x_d. Here t_s is the rise time.

The control strategy including filters and carrier signal algorithms are implemented digitally in the FORTRAN language. Data stored during the operation are transferred to a mainframe computer for further analysis.

Several experiments have been run to demonstrate the feasibility of our proposed control strategy. Figure 6 compares the measured displacement responses $x(t)$ for the conventional on-off control strategy and our approach based on the PWM control. The plot shows clearly that the system response is improved significantly in the PWM control. Figure 7 illustrates that as T_p is reduced, the average output from the PWM mode is very similar to that of a servo control, and consequently the displacement ripple is reduced as well. But as T_p is increased, the average output from the PWM mode is more like that from an on-off control with increased ripples. Accordingly, a small T_p is desired as the ripples and the steady-state error increase for a higher T_p. Finally Fig. 8 shows that for a smaller k_x, the system response is slower; and if k_x is too large, significant overshoot is seen.

7 Conclusions

The contributions of this research are as follows: (i) our method of varying only one pressure instead of two to drive the load reduces the system nonlinearity significantly which enables us to design the controller easily, (ii) an improved mathematical model incorporating pneumatic nonlinearities and nonlinear mechanical friction is developed for computer simulation studies and to guide laboratory experiments, and (iii) a method to overcome the nonlinear mechanical friction problem is proposed. Figure 9 compares step response $x(t)$ in the dimensionless form for both computer simulation and pneumatic robot experiment. Excellent agreement between prediction and measurement demonstrates that our proposed control strategy is indeed useful for an on-off valve controlled pneumatic system as it achieves a high position accuracy without using any mechanical stops. All of components used in the experiment described above are commercially available and hence it is possible to apply our proposed system to industrial automation. However, the role of several factors such as leakage, valve dynamic effects, and variation in friction must be understood well in order to design a robust controller. This study is currently in progress as a part of the long term research project on the dynamics and control of multidegree-of-freedom pneumatic robot.

References

Andersen, B. W., 1967, *The Analysis and Design of Pneumatic Systems*, John Wiley, New York.

Black, H. S., 1953, *Modulation Theory*, D. Van Nostrand, New York.

Botting, L. R., Eynon, G. T., and Foster, K., 1970, "The Response of a High-Pressure Pneumatic Servomechanism to Step and Sinewave Inputs," *Proc. Instn. Mech. Engrs.*, Vol. 184, No. 1, pp. 993-1012.

Bowns, D. E., and Ballard, R. L., 1972, "Digital Computation for the Analysis of Pneumatic Actuator System," *Proc. Instn. Mech. Engrs.*, Vol. 186, No. 73/72, pp. 881-889.

Burrows, C. R., and Webb, C. R., 1967, "Simulation of an On-off Pneumatic Servomechanism," *Proc. Instn. Mech. Engrs.*, Vol. 182, No. 1, p. 29.

Burrows, C. R., 1969, "Effect of Position on the Stability of Pneumatic Servomechanism," *J. Mechanical Engineering Science*, Vol. 11, No. 6, pp. 615-616.

Eun, T., Cho, H. S., and Cho, Y. J., 1982, "Stability and Positioning Accuracy of a Pneumatic On-off Servomechanism," *Proc. American Control Conference*, pp. 1189-1194.

Eun, T., Cho, H. S., and Lee, C. W., 1984, "On the Development of a Modified On-off Controller for Pneumatic Servo Mechanisms," *Proc. American Control Conference*, pp. 468-473.

Liu, S., and Bobrow, J. E., 1987, *An Analysis of a Pneumatic Servo System and its Application to a Computer-controlled Robot*, ASME Winter Meeting, DSC-Vol. 6, pp. 385-392.

Morita, Y. S., Shimizu, M., and Kagawa, T., 1985, "An Analysis on Pneumatic PWM and its Application to a Manipulator," *Proc. of International Symposium on Fluid Control and Measurement*, Tokyo, pp. 3-8.

Noritsugu, T., 1985, "Pulse-Width Modulated Feedback Force Control of a Pneumatically Powered Robot Hand," *Proc. of International Symposium on Fluid Control and Measurement*, Tokyo, pp. 47-52.

Noritsugu, T., 1987, "Development of PWM Mode Electro-Pneumatic Servomechanism Part II: Position Control of a Pneumatic Cylinder," *J. Fluid Control*, Vol. 66, pp. 65-80.

Scavarda, S., Kellal, A., and Richard, E., 1987, "Linearized Models for an Electropneumatic Cylinder Servovalve System," *Proc. of the 3rd International Conference in Advanced Robotics*, France, pp. 13-15.

Shearer, J. L., 1956, "Study of Pneumatic Process in the Continuous Control of Motion with Compressed Air-I and II," TRANS. ASME, pp. 233-242.

Shearer, J. L., 1957, "Nonlinear Analog Study of a High-Pressure Pneumatic Servomechanism," TRANS. ASME, pp. 465-472.